Published in final edited form as:
Synapse. 2009 July ; 63(7): 574–584. doi:10.1002/syn.20633.

PET Imaging of $D_{2/3}$ agonist binding in healthy human subjects with the radiotracer [^{11}C]-N-propyl-nor-apomorphine (NPA): preliminary evaluation and reproducibility studies

Rajesh Narendran[1,2], **W. Gordon Frankle**[1,2], **N. Scott Mason**[1], **Charles M. Laymon**[1], **Brian J Lopresti**, **Julie C. Price**[1], **Steve Kendro**[1], **Shivangi Vora**[1], **Maralee Litschge**[1], **James M. Mountz**[1], and **Chester A. Mathis**[1]

[1]Department of Radiology, University of Pittsburgh, Pittsburgh, PA

[2]Department of Psychiatry, University of Pittsburgh, Pittsburgh, PA

Abstract

Objective—(-)-N-[^{11}C]-Propyl-norapomorphine (NPA) is a full dopamine $D_{2/3}$ receptor agonist radiotracer suitable for imaging $D_{2/3}$ receptors configured in a state of high affinity for agonists using Positron Emission Tomography (PET). The aim of the present study was to define the optimal analytic method to derive accurate and reliable $D_{2/3}$ receptor parameters with [^{11}C]NPA.

Methods—Six healthy subjects (4 females/2 males) underwent two [^{11}C]NPA scans in the same day. $D_{2/3}$ receptor binding parameters were estimated using kinetic analysis (using 1- and 2- tissue compartment models) as well as simplified reference tissue method in the three functional subdivisions of the striatum (associative striatum, AST; limbic striatum LST and sensorimotor striatum SMST). The test-retest variability and intraclass correlation coefficient were assessed for distribution volume (V_T), binding potential relative to plasma concentration (BP_P), and binding potential relative to nondisplaceable uptake (BP_{ND})

Results—A two-tissue compartment kinetic model adequately described the functional subdivisions of the striatum as well as cerebellum time-activity data. The reproducibility of V_T was excellent (≤ 10%) in all regions, for this approach. The reproducibility of both BP_P (≤ 12%) and BP_{ND} (≤ 10%) was also excellent. The intraclass correlation coefficient of BP_P and BP_{ND} were acceptable as well (> 0.75) in the three functional subdivisions of the striatum. Although SRTM led to an underestimation of BP_{ND} values relative to that estimated by kinetic analysis by 8 to 13%, the values derived using both the methods were reasonably well correlated (r^2 = 0.89, n = 84). Both methods were similarly effective at detecting the differences in [^{11}C]NPA BP_{ND} between subjects.

Conclusion—The results of this study indicate that [^{11}C]NPA can be used to measure $D_{2/3}$ receptors configured in a state of high affinity for the agonists with high reliability and reproducibility in the functional subdivisions of the human striatum.

Keywords

PET; dopamine; [^{11}C]NPA; $D_{2/3}$ agonist

Correspondence Raj Narendran, MD University of Pittsburgh UPMC Presbyterian PET Facility, B938 200 Lothrop Street Pittsburgh, PA 15213 Phone: 412-647-5176 Fax: 412-647-0700 Email narendranr@upmc.edu.

Introduction

Like all G-protein linked receptors, dopamine $D_{2/3}$ receptors have been hypothesized to exist in two affinity states for agonists: the G-protein coupled high affinity state and the G-protein uncoupled low affinity state. Antagonist radiotracers such as [^{11}C]raclopride which are widely used to measure dopamine $D_{2/3}$ receptors bind with equal affinity to both the high and low affinity configuration of receptors and therefore do not distinguish between these two receptor affinity states (Roberts et al., 2004). In contrast, several recently introduced synthetic dopamine $D_{2/3}$ agonist radiotracers such as [^{11}C]NPA, [^{11}C]-methoxy-NPA (MNPA) and [^{11}C]PHNO provide us with the opportunity to selectively measure those $D_{2/3}$ receptors that are configured in a state of high affinity for the agonist in vivo.

The first of these radiotracers was the C-11 radiolabeled version of the full agonist N-propyl-norapomorphine (NPA), which was found to be suitable for the in vivo PET imaging of the $D_{2/3}$ receptors in non human primates (Hwang et al., 2000). Detailed characterization of [^{11}C]NPA in baboons revealed that [^{11}C]NPA binds with high affinity to a fraction (70 to 80%) of the sites labeled by [^{11}C]raclopride, suggesting that, in vivo, about 70 to 80% of $D_{2/3}$ receptors are configured in the high-affinity state for agonists (Narendran et al., 2005). Consistent with this observation, studies in non human primates have also documented that in vivo binding of [^{11}C]NPA is more vulnerable to endogenous competition than that of [^{11}C]raclopride by a factor of 1.42 (Narendran et al., 2004). Finally, in contrast to the $D_{2/3}$ agonist radiotracer [^{11}C]PHNO which demonstrates a relatively high preference to D_3 over D_2 receptors in humans (Graff-Guerrero et al., 2008), the in vivo binding profile of [^{11}C]NPA in baboons suggests comparable or slightly enhanced preference to D_3 receptors relative to the antagonist [^{11}C]raclopride (Narendran et al., 2006). Given its extensive preclinical characterization and in vivo binding profile suggesting it to be more comparable to [^{11}C]raclopride than [^{11}C]PHNO we were interested in evaluating [^{11}C]NPA in humans as it would allow for the study of in vivo dopamine $D_{2/3\ high}$ affinity agonist binding sites when contrasted with [^{11}C]raclopride.

The aim of this human PET study was to define the optimal analytical method for quantification of [^{11}C]NPA and to assess the reproducibility of $D_{2/3}$ receptor availability in the three functional subdivisions of the striatum as defined in (Martinez et al., 2003).

Methods

General Design

1. [^{11}C]NPA reproducibility studies

Human Subjects: The University of Pittsburgh Institutional Review Board and Radiation Human Use Subcommittee approved the study. In addition, the production and administration of [^{11}C]NPA to human subjects were performed under an Investigational New Drug Application (# 76, 327) submitted to the Food and Drug Administration. Six healthy volunteers participated in this study (age 32 ± 10 years, range 24 to 50, 2 males and 4 females; all non-smokers). The absence of pregnancy, medical, neurological and psychiatric history (including alcohol and drug abuse) was assessed by history, review of systems, physical examination, routine blood tests including pregnancy test, urine toxicology and EKG. All subjects provided written informed consent after receiving an explanation of the study.

Radiochemistry: [^{11}C]NPA was prepared using previously published methods (Hwang et al., 2000). The chemical purity of [^{11}C]NPA was 98.5% ± 2.5% and the radiochemical purity was 95.9% ± 2.5%.

PET protocol: Each subject underwent two scans with [^{11}C]NPA approximately three hours apart on the same day. An arterial catheter was inserted into the radial artery after completion of the Allen test and infiltration of the skin with 1% lidocaine. A venous catheter was inserted in a forearm vein on the opposite side. PET imaging was performed with the ECAT EXACT HR+ consistent with previously described image acquisition protocols (Abi-Dargham et al., 2000). A 10 min transmission scan was obtained prior to radiotracer injection. [^{11}C]NPA was injected i.v. over 45 sec. Emission data were collected in 3D mode for 90 min as 19 successive frames of increasing duration (4 × 15 s, 3 × 1 min, 3 × 2 min, 2 × 5 min, 7 × 10 min). Subjects were allowed to rest outside of the camera for approximately 45 to 60 min between the two injections.

Input function measurement: Following radiotracer injection, arterial samples were collected manually approximately every 6 seconds for the first two minutes and thereafter at longer intervals. A total of 35 samples were obtained per scan. Following centrifugation, plasma was collected in 200 μL aliquots and activities were counted in a gamma counter.

To determine the plasma activity representing unmetabolized parent compound of [^{11}C]NPA, seven samples (collected at 1, 4, 8, 12, 20, 40 and 60 min) were further processed using HPLC methods described previously (Hwang et al., 2004). The six measured parent fractions were fitted using a Hill model (Gunn et al., 1998).

The input function was then calculated as the product of total counts and interpolated parent fraction at each time point. The measured input function values were fitted to a sum of three exponentials from the time of peak plasma activity and the fitted values were used as the input to the kinetic analysis. The clearance of the parent compound (L/h) was calculated as the ratio of the injected dose to the area under the curve of the input function (Abi-Dargham et al., 1994).

For the determination of the plasma free fraction (f_P), triplicate aliquots of plasma collected prior to injection were mixed with the radiotracer, pipetted into ultrafiltration units (Amicon Centrifree; Millipore, Bedford, MA) and centrifuged at room temperature (30 min at 6000 rpm). At end of centrifugation, the plasma and ultrafiltrate activities were counted in a gamma counter, and f_P was calculated as the ratio of activity in the ultrafiltrate to total activity (Gandelman et al., 1994). Triplicate aliquots of saline solution mixed with the radiotracer were also processed, to determine the filter retention of the free tracer.

MRI acquisition: To provide an anatomical framework for analysis of the PET data, MRI scans were obtained using a 1.5 T GE Medical Systems (Milwaukee, WI) Signa Scanner and a 3D spoiled gradient recalled (SPGR) sequence was acquired in the coronal plane (TE/TR = 5/25, flip angle = 40 degree, NEX = 1, slice thickness = 1.5mm/0mm interslice).

Image analysis: PET data were reconstructed using filtered back-projection (Fourier rebinning/2D backprojection, 3 mm Hann filter) and corrected for photon attenuation (^{68}Ge/^{68}Ga rods), scatter, and radioactive decay. Reconstructed image files were then processed with the image analysis software MEDx (Sensor Systems, Inc., Sterling, Virginia) and SPM2 (www.fil.ion.ucl.ac.uk/spm). Frame-to-frame motion correction for head movement and MR-PET image alignment were performed using the mutual information algorithm implemented in SPM2. The drawing of regions of interest and generation of statistics for time activity curves were implemented in MEDx.

The striatum was divided into five anatomical subdivisions on the MRI using the criteria described in (Martinez et al., 2003). Mean region-of-interest volumes for the six subjects were:

1. Ventral striatum (VST, 2523 ± 475 mm^3)
2. Precommissural dorsal caudate (Pre-DCA, 3476 ± 693 mm^3),
3. Precommissural dorsal putamen (Pre-DPU, 2547 ± 433 mm^3),
4. Postcommissural caudate (Post CA, 1381 ± 400 mm^3) and
5. Postcommissural putamen (Post PU, 3804 ± 761 mm^3).

These anatomical subdivisions were then categorized into three functional subdivisions of the striatum:

1. the Limbic Striatum (LST), which includes the VST
2. the associative striatum (AST), which includes the Pre-DCA, Pre-DPU and Post CA and
3. the sensorimotor striatum (SMST), which includes the Post PU.

The outcome measure for the AST (7404 ± 1210 mm^3) was derived as a weighted average of the three anatomical subdivisions that comprised this region, while the outcome measure for the striatum (13731 ± 1812 mm^3) was derived as the weighted average of all five regions of interest.

Time activity curves were generated for the regions of interest using the criteria and methods outlined in (Martinez et al., 2003). The cerebellum (33539 ± 6832 mm^3) was sub sampled in fifteen consecutive coronal MRI slices caudal to the cerebellar penduncle and used as a reference region. The sub sampling included only the gray matter and excluded the vermis, white matter, and the cerebro-cerebellar fissure.

For bilateral regions, right and left values were averaged. The contribution of plasma total activity to the regional activity was calculated assuming a 5% blood volume in the regions of interest (Mintun et al., 1984) and tissue activities were calculated as the total regional activities minus the plasma contribution.

Quantitative analysis

Outcome measures: The three outcome measures provided are regional tissue distribution volume (V_T, mL cm^{-3}), binding potential relative to plasma concentration (BP_P, mL cm^{-3}) and binding potential relative to nonspecific uptake (BP_{ND}, unitless). The definition of these outcome measures are outlined in (Innis et al., 2007).

Derivation of distribution volumes

Kinetic Analysis: For the kinetic analyses both a two-compartment model (i.e. one tissue compartment, 1TC, 2-parameter model, K_1 and k_2) and a three-compartment model (i.e. two tissue compartment, 2TC, 4-parameter model, K_1 - k_4) were used. The 2TC model included the arterial plasma compartment (C_p), the intracerebral free and nonspecifically bound compartment (nondisplaceable compartment, C_{ND}), and the specifically bound compartment (C_S). The 1TC model included the arterial plasma compartment (C_P) and one tissue compartment (C_T) which includes both C_{ND} and C_S. The outcome parameter of interest is V_T, which was determined as either $V_T = K_1/k_2$ or $V_T = K_1/k_2(1+k_3/k_4)$ for the 1TC and 2TC models, respectively. The model parameters (k_i) were estimated using an established curve fitting technique that utilized the least squares minimization method (Levenberg, 1944) implemented as outlined in (Laruelle et al., 1994).

Model Order and Goodness of Fit: For the 1TC and 2TC, goodness of fit of models with different levels of complexity were compared using the Akaike Information Criterion (AIC,

Akaike, 1974), and the F test (Carson, 1986; Landlaw and DiStefano, 1984). The standard error of the parameters was given by the diagonal of the covariance matrix (Carson, 1986) and expressed as a percentage of the parameters (Identifiability, %Ident).

Determination of minimal scanning time: Experimental data were collected for 91 minutes. The minimal scanning time required to achieve time-independent derivation of regional striatal V_T was evaluated by fitting the time activity curves to shorter data sets, representing total scanning times of 81, 71, 61, 51 and 41 min, respectively. The resulting estimates of V_T were normalized to the V_T derived with the 91 minute data set. For each scan duration, the average and standard deviation of the eight normalized V_T were calculated. Time independence was considered achieved when two criteria were fulfilled (Huang et al., 2002): 1) the average normalized V_T was in between 95% and 105% of the reference V_T (small bias), and the 2) the SD of the normalized V_T is less than 10% (small error).

Simplified Reference Tissue Method (SRTM): To test the feasibility of quantification of [^{11}C]NPA BP_{ND} without collecting arterial plasma samples, the simplified reference tissue method (SRTM, Lammertsma and Hume, 1996) was implemented. In this approach, the arterial input function is not explicitly measured, but appears implicitly through its effect on a reference region. Because this method uses only brain data and not plasma data, BP_{ND} is the only receptor related parameter that can be estimated. The SRTM was implemented using an iterative optimization algorithm based upon the Levenberg-Marquart procedure with fitting weights proportional to frame duration (Frankle et al., 2006).

Evaluation of Methods: Results were evaluated according to two criteria: variability and reliability.

1) Variability. The test/retest variability was calculated as the absolute value of the difference between the test and retest, divided by the mean of the test and retest values.

2) Reliability. To evaluate the within-subject variability relative to the between-subject variability, both within-subject SD (WSSD) and between-subject SD (BSSD) were calculated and expressed as fraction of mean value (WS CV and BS CV). The reliability of the measurements was assessed by the intraclass correlation coefficient (ICC) calculated as (Kirk, 1982):

$$\frac{BSMSS - WSMSS}{BSMSS + (n-1)\,WSMSS}$$

where BSMSS is the mean sum of square between subjects, WSMSS is the mean sum of square within subjects and n is the number of repeated observations (n = 2 in this study). This statistic estimates the relative contributions of between and within subject variability and assumes values from -1 (i.e. BSMSS = 0) to 1 (identity between test and retest, i.e. WSMSS = 0). Given the relatively small number of subjects, n=6, the ICC may be of limited value in this application and needs to be interpreted with caution.

Statistical analysis: The average of the test and retest values were calculated for each subject (n = 6) and the results given as mean ± SD of these 6 average measurements. This allows for estimation of the variability in the population (i.e. between subject SD). When the SD refers to variability between experiments rather than between subjects, the SD is followed by n = 12. Dependent variables were analyzed using repeated measures ANOVA (RM ANOVA). A two-tailed probability value of 0.05 was selected as the significance level.

Relationships between outcome measures derived with different methods were evaluated by linear regressions.

Results

1. Reproducibility studies

Injected dose—The injected activity (9.8 ± 0.7 mCi or 363 ± 26 MBq, n = 12), injected mass (2.7 ± 0.6 μg, n = 12) and specific activity (1197 ± 401 Ci/mmol or 44.2 ± 14.8 MBq/nmol, n = 12) did not differ between the test and retest conditions (RM ANOVA, p = 0.59, 0.89 and 0.66, respectively).

Plasma analysis—After an initial, rapid distribution phase, total plasma activity stabilized at a relatively constant level (Figure 1; Right Panel). The percentage composition of plasma radioactivity over time is shown for [^{11}C]NPA in Figure 1 (Left Panel). At 20 minutes only 13% ± 3% of the total activity corresponded to the parent compound (mean across 6 subjects; Figure 1, Left panel). The average parent plasma clearance rate was 119 ± 36 L h^{-1}. The clearance rate for the test condition was not significantly different from that in the retest condition (117 ± 43 L h^{-1} vs. 119 ± 37 L h^{-1}, p = 0.87). The test/retest variability for the clearance was 20% ± 14% with an ICC = 0.62. The free fraction of [^{11}C]NPA in the plasma was 11% ± 2% and did not differ between conditions (p = 0.68); test/retest variability was 31% ± 22% with an ICC of 0.16.

Brain analysis—Representative brain time activity curves are shown in Figure 2. Activities in the cerebellum and striatum displayed early peaks (at ~ 3.5 min and ~ 8 min, respectively), followed by a rapid wash out.

Kinetic Analysis

Model order estimation: Both the 1TC and 2TC model reached convergence for every study in all regions (n = 6 subjects* 2 studies * 8 regions = 96 fits) with good identifiability (% Ident ≤ 5%). Representative fits for the 1 TC and 2 TC for the same brain time activity curve are shown in Figure 2. The models were compared for goodness of fit by the F test (Carson, 1986;Landlaw and DiStefano, 1984) and AIC (Akaike, 1974). The F test was significant ($p < 0.05$) in 61 out of the 96 fits examined, indicating that the higher order model (2TC) provided a better fit for 64% of the data sets. The AIC of the 2TC model was lower than the AIC of the 1TC in 76 of the 96 fits examined (79%), indicating a better fit. In all cases, when the F test indicated a better fit using the higher order model (61 out of 96), this was confirmed by the AIC. In general, the benefits of a 2 TC model were noticed to be highly significant (as indicated by a much lower p value) on both F test and AIC in the reference regions (cerebellum). Based on the model order estimation data the 2 TC was chosen as the model of choice for the kinetic analysis (data is only presented for this model hereafter and is referred to as kinetic analysis).

Table 1 lists the variability and ICC for $V_{T,}$ BP_P and BP_{ND} for the 2 TC kinetic analyses. The reproducibility and reliability for all three outcome measures $V_{T,}$ BP_P and BP_{ND} were excellent.

Determination of minimum scanning time: The maximum scanning time in all regions was 40 min, with the exception of Pre-DCA (50 min) and cerebellum (60 min). The cerebellum V_T was the rate limiting region, suggesting that the minimal scanning time for [^{11}C]NPA would need to be 60 min. An evaluation of the reproducibility of all three outcome measures V_T, BP_P and BP_{ND} obtained using the 60 min dataset was not significantly different than that observed with the 90 min dataset. Figure 3 displays the

biases and errors associated with shorter scan durations for each radiotracer in the striatum and cerebellum. An analysis of the data with SRTM yielded results that were consistent with the kinetic analysis in that the maximum scanning time in all regions was 40 min, with the exception of Pre-DCA (50 min) and Post-CA (50 min).

Simplified reference tissue method (SRTM) analysis—The results from the SRTM analyses are shown in Table 2 (A voxelwise BP_{ND} image generated for [^{11}C]NPA is contrasted with [^{11}C]raclopride in a representative subject in Figure 4). BP_{ND} derived by the SRTM was correlated with plasma input based BP_{ND} (SRTM v kinetic analysis, $y = 0.72x + 0.16$; $r^2 = 0.89$, $p < 0.0001$, $n = 84$). The BP_{ND} values in the striatal regions of interest derived via SRTM were on average 8.6% - 12.8% lower than those derived via the kinetic models. This difference was not statistically significant (RM ANOVA, $p = 0.24$). Also, in comparison to the kinetic model no differences were observed in the test/retest variability of [^{11}C]NPA BP_{ND} as measured with the SRTM method (RM ANOVA, $p = 0.62$).

Discussion

In this study, we report the first in human data derived by using the $D_{2/3}$ agonist radiotracer [^{11}C]NPA to image the functional subdivisions of the striatum. The primary objective of these studies was to define the optimal analytical strategy for derivation of the three outcome measures V_T, BP_P and BP_{ND} for [^{11}C]NPA and evaluate their reproducibility in healthy human subjects. Two kinetic analysis strategies were evaluated based on a specified compartmental configuration that utilizes the arterial time-activity curve as input function. Of the two compartmental models that were evaluated using this dataset for the kinetic analysis, the 2 TC model provided a significantly better fit for the regions of interest and reference region than did the 1 TC model. Thus, the 2 TC model was selected as the method of choice to analyze the data. Using the 2 TC model the reproducibility as measured by the test/retest variability of [^{11}C]NPA $V_{T,}$ BP_P and BP_{ND} was excellent (≤ 12%) in all regions.

In contrast to previous baboon studies (30% of the parent fraction was observed at 30 min post injection in baboons in Hwang et al., 2004), the percent parent of [^{11}C]NPA in plasma decreased more rapidly in humans (the percent of parent fraction at 30 min post injection was less than 13%). Consistent with this rapid decline in percent parent in plasma, the mean clearance of [^{11}C]NPA in humans (119 ± 36 L h^{-1}) was also significantly faster than that previously observed in baboons (29 ± 1 L h^{-1}). In addition, the plasma free fraction of [^{11}C]NPA in humans was determined to be around 11%, which was about twice as high as that observed in baboons (5%). Nevertheless, the striatal BP_{ND} of 0.9 ± 0.2 in humans was more or less in line with what was predicted from the [^{11}C]NPA baboon data (BPND = 1.16 ± 0.18, Hwang et al., 2004) following an adjustment for the 20-30% higher striatal $D_{2/3}$ B_{max} observed in non human primates.

Based on the initial evaluation of [^{11}C]NPA in humans, the following methodological considerations are discussed for future studies:

Signal to noise ratio

The average [^{11}C]NPA BP_{ND} (n =6 subjects) in the striatum was 0.9 ± 0.2. While the [^{11}C]NPA BP_{ND} values are significantly lower than that observed with the reference $D_{2/3}$ antagonist radiotracer [^{11}C]raclopride (average striatal BP_{ND} 2.6 ± 0.3, Mawlawi et al., 2001), it is nevertheless comparable to the values reported with other successful CNS PET/SPECT radioligands used in clinical studies (Table 3). Thus, the relatively lower BP_{ND} value compared to the antagonist [^{11}C]raclopride is unlikely to be a reason for concern in the study of $D_{2/3}$ agonist binding sites in health and disease. Nevertheless, it is possible that

the relatively low binding potential may limit the ability of [^{11}C]NPA as a superior probe to study amphetamine-induced DA release in the humans.

Reproducibility

As shown in Table 1, the test-retest variability of the three functional subdivisions (LST, AST and SMST) of the striatum was ≤ 10% for [^{11}C]NPA BP_{ND}. A slightly higher variance of ≤ 12% was observed for [^{11}C]NPA BP_P (Table 1). Thus, the reproducibility of [^{11}C]NPA in the functional subdivisions of the striatum is comparable to that reported for [^{11}C]raclopride (BP_{ND} ≤ 10% and BP_P ≤ 12%) in (Mawlawi et al., 2001). Therefore, a measurement bias due to differences in radiotracer reproducibility is unlikely to be observed in using these radioligands to contrast $D_{2/3}$ agonist and antagonist binding sites in the functional subdivisions of the striatum in human subjects.

[^{11}C]NPA receptor occupancy

To calculate the in vivo receptor occupancy at the mass doses (< 5 μg) injected in the reproducibility studies we assumed the in vivo K_D of [^{11}C]NPA in humans was identical to that in non human primates (0.16 nM) (Narendran et al., 2005). We measured the concentration of [^{11}C]NPA in the cerebellum at the time of peak specific binding (8 ± 3 min), and multiplied this value by f_{ND}, to obtain an estimate of the free brain concentration (F) at time of peak specific binding. f_{ND} was calculated as f_P/V_{TCER}, and was 3% ± 1%. The occupancy was calculated as $100*F/(K_D+F)$ and regressed against the injected mass (see Figure 5). Based on these data, the injected mass of [^{11}C]NPA will necessarily need to be restricted to ≤ 2 μg to ensure the assumption of tracer dose (< 5% receptor occupancy) is not violated. The two to three fold lower injected mass limit in humans (≤ 2 μg) is consistent with the much higher f_{ND} observed in humans (3 ± 1%) relative to baboons (1 ± 0.3%) (Narendran et al., 2005). Based on the specific activities of our preliminary studies, a maximum injected radioactivity dose of 6-8 mCi is likely to be accomplished with this ≤ 2 μg mass limit. An injected radioactivity dose range of 6-8 mCi while a bit on the lower end for PET studies, has been shown to be adequate for imaging with other [C-11] PET radioligands such as [^{11}C]raclopride, [^{11}C]WAY and [^{11}C]FLB457 (Boileau et al., 2007; Parsey et al., 2000; Sudo et al., 2001).

Scanning duration

As the V_T in the cerebellum and striatal subregions were stable at 60 minutes it is likely that future clinical studies could restrict the [^{11}C]NPA PET data acquisition to this time frame.

SRTM analysis with no arterial blood input

Although the BP_{ND} values derived using SRTM were lower they were reasonably well correlated with the values derived using the kinetic analysis. An issue of concern was that the regression of the SRTM BP_{ND} to kinetic BP_{ND} had a slope less than unity (0.72) and a slightly positive intercept (0.17), which is suggestive of a more pronounced underestimation of BP_{ND} values in regions of higher receptor density relative to that in regions of low receptor density. A similar phenomenon has been reported previously for the 5HT1A receptor antagonist radiotracer [^{11}C]WAY 100635 and the implications of the use of reference tissue methods in clinical studies have been discussed extensively in (Parsey et al., 2000). Thus, the use of SRTM as a preferred method for the quantification of [^{11}C]NPA in clinical populations will need to be considered with caution until this issue is further understood in larger data sets.

Preferential binding to D_3 receptors

We were interested in evaluating the binding of [^{11}C]NPA in the globus pallidus (GP), a region relatively enriched with D_3 receptors as previous studies with another dopamine $D_{2/3}$ agonist radiotracer [^{11}C]PHNO have demonstrated its preferential binding to D_3 relative to D_2 receptors in the GP (Narendran et al., 2006). The fractional binding in the D_3-enriched GP relative to the D_3-devoid dorsal striatum (DST, derived as weighted average of AST and SMST) has been used in previous studies to contrast the preference of [^{11}C]raclopride, [^{11}C]NPA and [^{11}C]PHNO to bind to D_3 relative to D_2 receptors (Narendran et al., 2006). As three of the six subjects who participated in the [^{11}C]NPA PET studies had also been scanned with [^{11}C]raclopride within the past six months under a different research protocol it allowed for the direct comparison of the binding potential (BP_{ND}) of these two radiotracers in the globus pallidus and dorsal striatum. For this particular analysis we subsampled the globus pallidus on the same coronal slices adjacent to the Post PU. The medial and lateral boundary of this region were defined by the posterior limb of the internal capsule and Post PU respectively using criteria outlined in (Ifthikharuddin et al., 2000). The average [^{11}C]raclopride binding in the GP and DST in the n=3 subjects was 1.51 ± 0.14 and 2.59 ± 0.45. The average [^{11}C]NPA binding in the GP and DST in the same three subjects was 0.82 ± 0.06 and 0.87 ± 0.04. Thus, the ratio of the D_3-enriched GP to the D_3-devoid DST was much higher for [^{11}C]NPA (98%) compared to [^{11}C]raclopride (58%). Despite the fact that the measured fraction of binding in the D_3 receptor enriched GP was not as high as that observed with another $D_{2/3}$ agonist radiotracer [^{11}C]PHNO ([^{11}C]PHNO BP_{ND} GP/DST =187%; Narendran et al., 2006) the available data is still suggestive of [^{11}C]NPA having a slightly higher preference for D_3 receptors than [^{11}C]raclopride. This observation is consistent with some (Kula et al., 1994; Sautel et al., 1995) but not all (Freedman et al., 1994; Seeman et al., 2005) in vitro data that suggest [^{11}C]NPA has slightly enhanced preference for D_3 relative to D_2 receptors (see Table 1 in Narendran et al., 2006). Thus, in a clinical study contrasting $D_{2/3}$ agonist versus $D_{2/3}$ antagonist binding the difference between [^{11}C]NPA BP and [^{11}C]raclopride BP will be influenced not only by the agonist versus antagonist binding properties but also the D_3 versus D_2 K_D differential. Therefore, the influence of both these two pharmacological variables will need to be accounted for in the interpretation of the data.

Physiological effects/ safety profile of [^{11}C]NPA in humans

To date 23 injections have been performed in 13 subjects with an injected mass of [^{11}C]NPA ≤ 5 μg under a Food and Drug Administration Investigational New Drug Protocol (includes both dosimetry and test-retest studies conducted at the University of Pittsburgh PET Facility). No significant changes in blood pressure, heart rate, EKG, physical/neurological exam were observed (data submitted and reviewed by the Food and Drug Administration as part of the [^{11}C]NPA Investigational New Drug Annual Report). Of particular note was the lack of nausea or vomiting in the [^{11}C]NPA studies. This adverse effect was reported in a third of the subjects receiving another novel $D_{2/3}$ agonist radiotracer, [^{11}C]PHNO (14 out of 43 injections in twenty subjects, Willeit et al., 2008). It is likely that the relatively rapid brain and plasma clearance, lower free fraction in plasma and less affinity for D_3 receptors contribute to the better tolerance (or lack of nausea and vomiting) of [^{11}C]NPA compared to [^{11}C]PHNO.

Conclusion

The results of this study indicate that [^{11}C]NPA can be used to reliably measure $D_{2/3}$ receptors configured in a state of high affinity for the agonists in humans. Although the [^{11}C]NPA BP_{ND} is relatively low compared to the reference $D_{2/3}$ antagonist [^{11}C]raclopride and another $D_{2/3}$ agonist [^{11}C]PHNO, it demonstrated an excellent test-retest variability that

was comparable to that observed with these other $D_{2/3}$ imaging agents in humans (Mawlawi et al., 2001; Willeit et al., 2005). Initial in vivo PET studies in humans also suggest that the agonist [^{11}C]NPA may exhibit a slightly higher preference for D_3 receptors than the antagonist [^{11}C]raclopride. This is likely to confound the interpretation of contrasting agonist and antagonist binding potential in human studies, especially in striatal regions that are relatively enriched with D_3 receptors such as the ventral striatum. Nevertheless, the use of [^{11}C]NPA as a PET radiotracer in humans is likely to inform us of the in vivo status of D_{2high} and D_{3high} receptor states in the functional subdivisions of the striatum in both health and disease.

Acknowledgments

The authors thank members of the PET Facility Staff who carried out the acquisition of PET data and care of all subjects during PET procedures. The authors also acknowledge the editorial assistance provided by Maureen A. May, BS.

This work was supported by an NIMH Career Development Award to Dr. Narendran (1-K08 MH 068762-03) and the University of Pittsburgh Department of Radiology. As this article was supported by US Government funds it is in the public domain in the United States of America.

References

Abi-Dargham A, Laruelle M, Seibyl J, Rattner Z, Baldwin RM, Zoghbi SS, Zea-Ponce Y, Bremner JD, Hyde TM, Charney DS, Hoffer PB, Innis RB. SPECT measurement of benzodiazepine receptors in human brain with [123-I]iomazenil: kinetic and equilibrium paradigms. J Nucl Med. 1994; 35:228–238. [PubMed: 8294990]

Abi-Dargham A, Martinez D, Mawlawi O, Simpson N, Hwang DR, Slifstein M, Anjilvel S, Pidcock J, Guo NN, Lombardo I, Mann JJ, Van Heertum R, Foged C, Halldin C, Laruelle M. Measurement of striatal and extrastriatal dopamine D1 receptor binding potential with [11C]NNC 112 in humans: validation and reproducibility. J Cereb Blood Flow Metab. 2000; 20(2):225–243. [PubMed: 10698059]

Akaike H. A new look at the statistical model identification. IEEE Trans Automat Contr AC. 1974; 19:716–723.

Boileau I, Dagher A, Leyton M, Welfeld K, Booij L, Diksic M, Benkelfat C. Conditioned dopamine release in humans: a positron emission tomography [11C]raclopride study with amphetamine. J Neurosci. 2007; 27(15):3998–4003. [PubMed: 17428975]

Carson, RE. Parameters estimation in positron emission tomography. In: Phelps, ME.; Mazziotta, JC.; Schelbert, HR., editors. Positron emission tomography Principles and applications for the brain and the heart. Raven Press; New York: 1986. p. 347-390.

Ding YS, Fowler JS, Volkow ND, Dewey SL, Wang GJ, Logan J, Gatley SJ, Pappas N. Chiral drugs: comparison of the pharmacokinetics of [11C]d-threo and L-threo-methylphenidate in the human and baboon brain. Psychopharmacology (Berl). 1997; 131(1):71–78. [PubMed: 9181638]

Frankle WG, Huang Y, Hwang DR, Talbot PS, Slifstein M, Van Heertum R, Abi-Dargham A, Laruelle M. Comparative evaluation of serotonin transporter radioligands 11C-DASB and 11C-McN 5652 in healthy humans. J Nucl Med. 2004; 45(4):682–694. [PubMed: 15073266]

Frankle WG, Slifstein M, Gunn RN, Huang Y, Hwang DR, Darr EA, Narendran R, Abi-Dargham A, Laruelle M. Estimation of Serotonin Transporter Parameters with 11C-DASB in Healthy Humans: Reproducibility and Comparison of Methods. J Nucl Med. 2006; 47(5):815–826. [PubMed: 16644752]

Freedman SB, Patel S, Marwood R, Emms F, Seabrook GR, Knowles MR, McAllister G. Expression and pharmacological characterization of the human D3 dopamine receptor. J Pharmacol Exp Ther. 1994; 268(1):417–426. [PubMed: 8301582]

Gandelman MS, Baldwin RM, Zoghbi SS, Zea-Ponce Y, Innis RB. Evaluation of ultrafiltration for the free fraction determination of single photon emission computerized tomography (SPECT) radiotracers: β-CIT, IBF and iomazenil. J Pharmaceutical Sci. 1994; 83:1014–1019.

Graff-Guerrero A, Willeit M, Ginovart N, Mamo D, Mizrahi R, Rusjan P, Vitcu I, Seeman P, Wilson AA, Kapur S. Brain region binding of the D(2/3) agonist [(11)C]-(+)-PHNO and the D(2/3) antagonist [(11)C]raclopride in healthy humans. Hum Brain Mapp. 2008; 29(4):400–410. [PubMed: 17497628]

Gunn RN, Sargent PA, Bench CJ, Rabiner EA, Osman S, Pike VW, Hume SP, Grasby PM, Lammertsma AA. Tracer kinetic modeling of the 5-HT1A receptor ligand [carbonyl-11C]WAY-100635 for PET. Neuroimage. 1998; 8(4):426–440. [PubMed: 9811559]

Huang Y, Hwang DR, Narendran R, Sudo Y, Chatterjee R, Bae SA, Mawlawi O, Kegeles LS, Wilson AA, Kung HF, Laruelle M. Comparative Evaluation in Nonhuman Primates of Five PET Radiotracers for Imaging the Serotonin Transporters: [11C]McN 5652, [11C]ADAM, [11C]DASB, [11C]DAPA, and [11C]AFM. J Cereb Blood Flow Metab. 2002; 22(11):1377–1398. [PubMed: 12439295]

Hwang D, Kegeles LS, Laruelle M. (-)-N-[(11)C]propyl-norapomorphine: a positron-labeled dopamine agonist for PET imaging of D(2) receptors. Nucl Med Biol. 2000; 27(6):533–539. [PubMed: 11056366]

Hwang DR, Narendran R, Huang Y, Slifstein M, Talbot PS, Sudo Y, Van Berckel BN, Kegeles LS, Martinez D, Laruelle M. Quantitative Analysis of (-)-N-(11)C-Propyl-Norapomorphine In Vivo Binding in Nonhuman Primates. J Nucl Med. 2004; 45(2):338–346. [PubMed: 14960658]

Ifthikharuddin SF, Shrier DA, Numaguchi Y, Tang X, Ning R, Shibata DK, Kurlan R. MR volumetric analysis of the human basal ganglia: normative data. Acad Radiol. 2000; 7(8):627–634. [PubMed: 10952114]

Innis RB, Cunningham VJ, Delforge J, Fujita M, Gjedde A, Gunn RN, Holden J, Houle S, Huang SC, Ichise M, Iida H, Ito H, Kimura Y, Koeppe RA, Knudsen GM, Knuuti J, Lammertsma AA, Laruelle M, Logan J, Maguire RP, Mintun MA, Morris ED, Parsey R, Price JC, Slifstein M, Sossi V, Suhara T, Votaw JR, Wong DF, Carson RE. Consensus nomenclature for in vivo imaging of reversibly binding radioligands. J Cereb Blood Flow Metab. 2007; 27(9):1533–1539. [PubMed: 17519979]

Kegeles LS, Zea-Ponce Y, Abi-Dargham A, Rodenhiser J, Wang T, Weiss R, Van Heertum RL, Mann JJ, Laruelle M. Stability of [123I]IBZM SPECT measurement of amphetamine-induced striatal dopamine release in humans. Synapse. 1999; 31(4):302–308. [PubMed: 10051112]

Kirk, RE. Experimental design: procedures for the behavioral sciences. Brooks/Cole publishing company; Pacific Grove, California: 1982.

Kula NS, Baldessarini RJ, Kebabian JW, Neumeyer JL. S-(+)-aporphines are not selective for human D3 dopamine receptors. Cell Mol Neurobiol. 1994; 14(2):185–191. [PubMed: 7842476]

Lammertsma AA, Hume SP. Simplified reference tissue model for PET receptor studies. Neuroimage. 1996; 4(3 Pt 1):153–158. [PubMed: 9345505]

Landlaw EM, DiStefano JJ III. Multiexponential, multicompartmental, and noncompartmental modeling. II. Data analysis and statistical considerations. Am J Physiol. 1984; 246:R665–R677. [PubMed: 6720989]

Laruelle M, Wallace E, Seibyl JP, Baldwin RM, Zea-Ponce Y, Zoghbi SS, Neumeyer JL, Charney DS, Hoffer PB, Innis RB. Graphical, kinetic and equilibrium analysis of [^{123}I]β-CIT in vivo binding to dopamine transporters in healthy subjects. J Cereb Blood Flow Metab. 1994; 14:982–994. [PubMed: 7929662]

Levenberg K. A method for the solution of certain problems in least squares. Quart Appl Math. 1944; 2:164–168.

Martinez D, Slifstein M, Broft A, Mawlawi O, Hwang DR, Huang Y, Cooper T, Kegeles L, Zarahn E, Abi-Dargham A, Haber SN, Laruelle M. Imaging human mesolimbic dopamine transmission with positron emission tomography. Part II: amphetamine-induced dopamine release in the functional subdivisions of the striatum. J Cereb Blood Flow Metab. 2003; 23(3):285–300. [PubMed: 12621304]

Mawlawi O, Martinez D, Slifstein M, Broft A, Chatterjee R, Hwang DR, Huang Y, Simpson N, Ngo K, Van Heertum R, Laruelle M. Imaging human mesolimbic dopamine transmission with positron emission tomography: I. Accuracy and precision of D2 receptor parameter measurements in ventral striatum. J Cereb Blood Flow Metab. 2001; 21(9):1034–1057. [PubMed: 11524609]

Mintun MA, Raichle ME, Kilbourn MR, Wooten GF, Welch MJ. A quantitative model for the in vivo assessment of drug binding sites with positron emission tomography. Ann Neurol. 1984; 15:217–227. [PubMed: 6609679]

Narendran R, Hwang DR, Slifstein M, Hwang Y, Huang Y, Ekelund J, Guillin O, Scher E, Martinez D, Laruelle M. Measurement of the proportion of D2 receptors configured in state of high affinity for agonists in vivo: a positron emission tomography study using [11C]N-propylnorapomorphine and [11C]raclopride in baboons. J Pharmacol Exp Ther. 2005; 315(1):80–90. [PubMed: 16014571]

Narendran R, Hwang DR, Slifstein M, Talbot PS, Erritzoe D, Huang Y, Cooper TB, Martinez D, Kegeles LS, Abi-Dargham A, Laruelle M. In vivo vulnerability to competition by endogenous dopamine: Comparison of the D2 receptor agonist radiotracer (-)-N-[11C]propyl-norapomorphine ([11C]NPA) with the D2 receptor antagonist radiotracer [11C]-raclopride. Synapse. 2004; 52(3): 188–208. [PubMed: 15065219]

Narendran R, Slifstein M, Guillin O, Hwang Y, Hwang D-R, Scher E, Reeder S, Rabiner EA, Laruelle M. The dopamine (D2/3) receptor agonist PET radiotracer [11C]-(+)-PHNO is a D3 receptor preferring agonist in vivo. Synapse. 2006; 60(7):485–495. [PubMed: 16952157]

Okubo Y, Suhara T, Suzuki K, Kobayashi K, Inoue O, Terasaki O, Someya Y, Sassa T, Sudo Y, Matsushima E, Iyo M, Tateno Y, Toru M. Decreased prefrontal dopamine D1 receptors in schizophrenia revealed by PET. Nature. 1997; 385(6617):634–636. [PubMed: 9024661]

Parsey RV, Slifstein M, Hwang DR, Abi-Dargham A, Simpson N, Mawlawi O, Guo NN, Van Heertum R, Mann JJ, Laruelle M. Validation and reproducibility of measurement of 5-HT1A receptor parameters with [carbonyl-11C]WAY-100635 in humans: comparison of arterial and reference tissue input functions. J Cereb Blood Flow Metab. 2000; 20(7):1111–1133. [PubMed: 10908045]

Roberts DJ, Lin H, Strange PG. Mechanisms of agonist action at D2 dopamine receptors. Mol Pharmacol. 2004; 66(6):1573–1579. [PubMed: 15340043]

Sautel F, Griffon N, Levesque D, Pilon C, Schwartz JC, Sokoloff P. A functional test identifies dopamine agonists selective for D3 versus D2 receptors. Neuroreport. 1995; 6(2):329–332. [PubMed: 7756621]

Seeman P, Ko F, Willeit M, McCormick P, Ginovart N. Antiparkinson concentrations of pramipexole and PHNO occupy dopamine D2(high) and D3(high) receptors. Synapse. 2005; 58(2):122–128. [PubMed: 16088951]

Smith GS, Price JC, Lopresti BJ, Huang Y, Simpson N, Holt D, Mason NS, Meltzer CC, Sweet RA, Nichols T, Sashin D, Mathis CA. Test-retest variability of serotonin 5-HT2A receptor binding measured with positron emission tomography and [18F]altanserin in the human brain [In Process Citation]. Synapse. 1998; 30(4):380–392. [PubMed: 9826230]

Sudo Y, Suhara T, Inoue M, Ito H, Suzuki K, Saijo T, Halldin C, Farde L. Reproducibility of [11 C]FLB 457 binding in extrastriatal regions. Nucl Med Commun. 2001; 22(11):1215–1221. [PubMed: 11606887]

Wang GJ, Volkow ND, Fowler JS, Fischman M, Foltin R, Abumrad NN, Logan J, Pappas NR. Cocaine abusers do not show loss of dopamine transporters with age. Life Sci. 1997; 61(11):1059–1065. [PubMed: 9307051]

Willeit M, Ginovart N, Graff A, Rusjan P, Vitcu I, Houle S, Seeman P, Wilson AA, Kapur S. First human evidence of d-amphetamine induced displacement of a D2/3 agonist radioligand: A [11C]-(+)-PHNO positron emission tomography study. Neuropsychopharmacology. 2008; 33(2):279–289. [PubMed: 17406650]

Willeit M, Ginovart N, Kapur S, Houle S, Hussey D, Seeman P, Wilson AA. High-Affinity States of Human Brain Dopamine D2/3 Receptors Imaged by the Agonist [(11)C]-(+)-PHNO. Biol Psychiatry. 2005

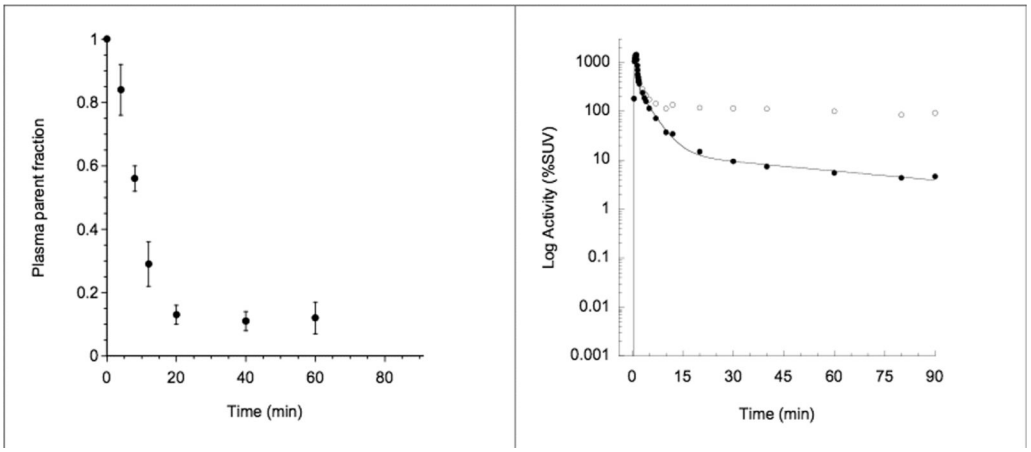

Figure 1.

[^{11}C]NPA Plasma Analysis. Left panel: mean ± SD fraction of plasma activity corresponding to parent compound over time (n = 6 subjects measured twice). Right panel: typical plasma time-activity curve measured in one experiment. Open circles are measured activities, closed circles are measured activities corrected for metabolites, and the line is a three-exponential fit to the measured, metabolite-corrected values. Fitted values were used as input function for the kinetic analysis of brain time-activity curves.

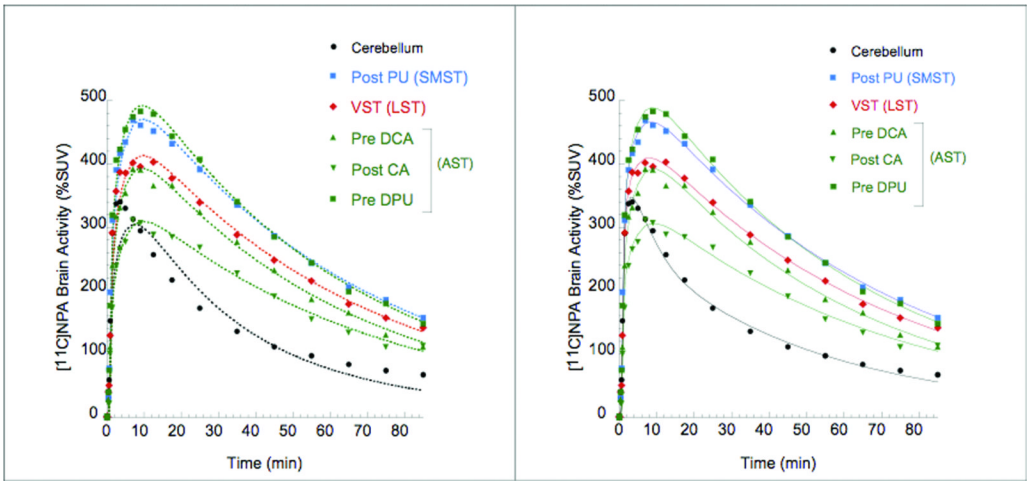

Figure 2.

[^{11}C]NPA time activity curves in cerebellum (black circles) and striatal subdivisions (as defined in Martinez et al 2003) Points are measured values. Left panel shows the line fitted to a 1-tissue compartment model. Right panel shows the line fitted to a 2-tissue compartment model. The 2 TC model provided significantly better fits both in the cerebellum and other regions of interest.

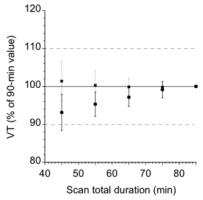

Figure 3.

Time stability of [^{11}C]NPA V_T in the striatum (squares) and cerebellum (circles). Times refer to the midpoint of each 10-min acquisition. Data of shorter duration were analyzed, and estimated V_T (mean ± SD) is expressed as a percentage of the value derived with the complete data set (90 min). Each point is the average of 12 scans. Deviation from 100% of mean value indicates bias associated with shorter scanning times, whereas SD indicates error associated with shorter scanning times.

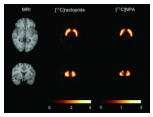

Figure 4.
Parametric BP_{ND} maps measured in a 24 year old female under baseline conditions following [^{11}C]raclopride and [^{11}C]NPA. Parametric maps were obtained by derivation of BP_{ND} in each voxel by SRTM analysis. Because [^{11}C]raclopride BP_{ND} is larger than [^{11}C]NPA BP_{ND}, it was not possible to display both ligands with the same color scale. For each ligand, the range of the color scale was set at twice the baseline BP_{ND} value measured in these scans.

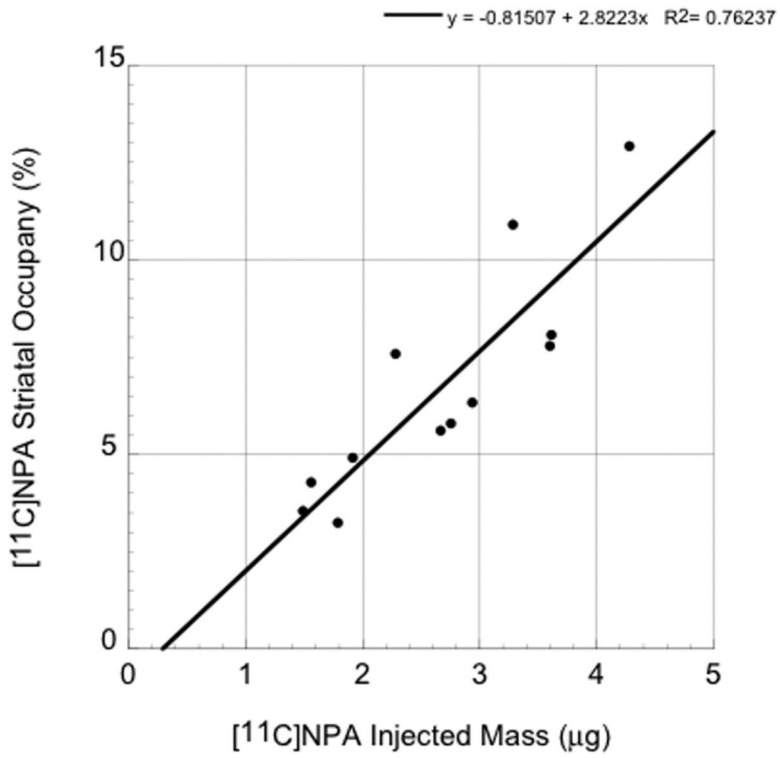

Figure 5.
Relationship between injected mass (x axis, µg) and peak occupancy in striatum (y-axis, %) of [^{11}C]NPA achieved in 12 human scans. Based on these data a [^{11}C]NPA injected mass of ≤ 2 µg provides a peak striatal occupancy of < 5%

Table 1

Reproducibility of [11C]NPA total distribution volume (V_t, mL cm^{-3}), binding potential relative to plasma concentrations (BP_p, mL cm^{-3}) and binding potential relative to non specific uptake (BP_{nd}, unitless) derived via kinetic analysis (2 TC)

		V_T (mL cm^{-3})					BP_P (mL cm^{-3})					BP_{ND}				
Subdivision	**Region**	**Mean**	**(BSSD CV)**	**(WSSD CV)**	**VAR + SD**	**ICC**	**Mean**	**(BSSD CV)**	**(WSSD CV)**	**VAR + SD**	**ICC**	**Mean**	**(BSSD CV)**	**(WSSD CV)**	**VAR + SD**	**ICC**
	Cerebellum	4.03	(0.06)	(0.04)	6% ± 4%	0.52	-	-	-	-	-	-	-	-	-	-
LST	VST	7.26	(0.15)	(0.05)	7% ± 7%	0.78	3.23	(0.30)	(0.08)	9% ± 9%	0.87	0.80	(0.28)	0.04	5% ± 5%	0.95
AST		7.35	(0.14)	(0.04)	8% ± 3%	0.83	3.32	(0.28)	(0.06)	10% ± 3%	0.92	0.82	(0.26)	0.03	5% ± 4%	0.97
	Pre-DCA	7.10	(0.13)	(0.04)	7% ± 3%	0.82	3.07	(0.26)	(0.06)	8% ± 6%	0.91	0.76	(0.24)	0.04	7% ± 4%	0.94
	Pre-DPU	8.21	(0.15)	(0.05)	9% ± 5%	0.80	4.18	(0.28)	(0.07)	12% ± 7%	0.88	1.04	(0.26)	0.04	8% ± 5%	0.95
	Post-CA	6.31	(0.11)	(0.04)	7% ± 5%	0.73	2.28	(0.26)	(0.08)	12% ± 7%	0.85	0.56	(0.25)	0.06	10% ± 9%	0.88
SMST	Post-PU	8.40	(0.13)	(0.06)	9% ± 5%	0.78	4.36	(0.22)	(0.08)	12% ± 6%	0.78	1.08	(0.19)	0.04	6% ± 4%	0.91
STR		7.61	(0.14)	(0.05)	8% ± 4%	0.79	3.58	(0.25)	(0.06)	10% ± 4%	0.89	0.89	(0.23)	0.03	4% ± 3%	0.98

Values are the mean of 6 subjects with each value measured twice. BSSD CV = between subject standard deviation coefficient of variation, WSSD CV = within subject standard deviation coefficient of variation, VAR = test/retest variation, ICC = intraclass correlation coefficient.

Synapse. Author manuscript; available in PMC 2010 July 1.

Table 2

Reproducibility of [^{11}C]NPA binding potential relative to non specific uptake (BP_{ND}, unitless) as derived via SRTM analysis

Subdivision	Region	Mean	(BSSD CV)	(WSSDCV)	VAR + SD	ICC
LST	VST	0.71	(0.20)	(0.04)	7% ± 3%	0.93
AST		0.75	(0.17)	(0.04)	6% ± 4%	0.90
	Pre-DCA	0.69	(0.15)	(0.05)	7% ± 7%	0.79
	Pre-DPU	0.95	(0.18)	(0.04)	8% ± 5%	0.89
	Post-CA	0.50	(0.22)	(0.06)	10% ± 7%	0.85
SMST	Post-PU	0.99	(0.10)	(0.03)	6% ± 1%	0.81
STR		0.81	(0.15)	(0.03)	4% ± 4%	0.94

Values are the mean of 6 subjects with each value measured twice. BSSD CV = between subject standard deviation coefficient of variation, WSSD CV = within subject standard deviation coefficient of variation, VAR = test/retest variation, ICC = intraclass correlation coefficient.

Table 3

CNS PET/SPECT radioligands with relatively lower BP_{ND} values

Radioligand	Region of Interest	BP_{ND}	Reference
[123I]IBZM	Striatum	0.7 ± 0.1	(Kegeles et al., 1999)
[^{11}C]cocaine	Striatum	0.8 ± 0.1	(Wang et al., 1997)
[^{11}C]-d-threo-methylphenidate	Striatum	1.5 ± 0.3	(Ding et al., 1997)
[^{11}C]NNC 112	Prefrontal cortex	0.8 ± 0.3	(Abi-Dargham et al., 2000)
[^{11}C]SCH 23390	Prefrontal cortex	0.4 ± 0.1	(Okubo et al., 1997)
[^{18}F]altanserin	Cortical ROI	0.7 to 1.5	(Smith et al., 1998)
[^{11}C] McNeil 5652	Midbrain	1.2 ± 0.3	(Frankle et al., 2004)
	Striatum Subdivisions	0.7 to 1.0	(Frankle et al., 2004)
[^{11}C]NPA	**Striatum Subdivisions**	**0.8 to 1.1**	**This study**